Sensors and Actuators B 198 (2014) 472–478

Contents lists available at ScienceDirect

Sensors and Actuators B: Chemical

journal homepage: www.elsevier.com/locate/snb

A paper-based oxygen generating platform with spatially defined catalytic regions☆

Manuel Ochoa[a,*], Rahim Rahimi[a], Tiffany L. Huang[b], Neslihan Alemdar[c,d], Ali Khademhosseini[c,d,e,f,g], Mehmet R. Dokmeci[c,d], Babak Ziaie[a]

[a] School of Electrical and Computer Engineering, Purdue University, West Lafayette, IN, USA
[b] Department of Bioengineering, Rice University, Houston, TX, USA
[c] Center for Biomedical Engineering, Department of Medicine, Brigham and Women's Hospital, Harvard Medical School, Cambridge, MA 02139, USA
[d] Harvard-MIT Division of Health Sciences and Technology, Massachusetts Institute of Technology, Cambridge, MA 02139, USA
[e] Wyss Institute for Biologically Inspired Engineering, Harvard University, Boston, MA 02115, USA
[f] Department of Maxillofacial Biomedical Engineering and Institute of Oral Biology, School of Dentistry, Kyung Hee University, Seoul 130-701, Republic of Korea
[g] Department of Physics, King Abdulaziz University, Jeddah 21569, Saudi Arabia

ARTICLE INFO

Article history:
Received 1 October 2013
Received in revised form
25 December 2013
Accepted 5 February 2014
Available online 24 February 2014

Keywords:
Oxygen generation
Parchment paper
Wound healing
Hydrogen peroxide
Manganese dioxide

ABSTRACT

A flexible, parchment paper/PDMS based platform for local wound oxygenation is fabricated and characterized. The platform consists of a PDMS microfluidic network bonded to a parchment paper substrate. Generation of oxygen occurs by flowing H_2O_2 through the channels and chemically decomposing it via a catalyst embedded in laser-defined regions of the parchment paper. PDMS is bonded to parchment paper using partially cured PDMS followed by a brief air plasma treatment, resulting in a strong bond. For pressures below 110 Torr the parchment paper is observed to be impermeable to water and hydrogen peroxide. The oxygen permeability of parchment paper is measured to be 1.42 μL/(Torr mm^2 min). Using a peroxide flow rate of 250 μL/min, oxygen generation in the catalyst spots raises the oxygen level on the opposite side of the parchment paper from atmospheric levels (21%) to 25.6%, with a long-term (30 h) generation rate of 0.1 μL O_2/min/mm^2. This rate is comparable to clinically proven levels for adequate healing. Device and material *in vitro* biocompatibility is confirmed with NIH 3T3 fibroblast cells via alamar blue assays.

1. Introduction

Suboptimal oxygenation of the wound bed is a major healing inhibitor in chronic wounds [1–4]. A chronic wound is one which does not heal in an orderly or timely manner (i.e. three months) due to an inadequate healing microenvironment. Unlike acute injuries that receive sufficient oxygen via a functional blood vessel network, chronic wounds often suffer from a lack of a proper vascular network incapable of providing sufficient oxygen for tissue growth. While the lack of oxygen may trigger vascular regeneration [5], the severity and depth of wounds can prevent adequate regeneration, causing wound ischemia [6].

Modern medical treatment of hypoxic chronic wounds typically employs hyperbaric oxygen therapy [7–11], which requires bulky equipment and often exposes large areas of the body to unnecessarily elevated oxygen concentrations that can damage healthy tissue. Hence, such methods require very careful and periodic oxygen administration to avoid hyper-oxygenation of tissue surrounding the wound. In a more practical approach, recent research has endorsed transdermal oxygen therapy (TOT) as a viable and effective method for oxygenating a hypoxic wound [12–16]. A variety of wound dressings can be used to create an enclosure around a wound which can entrap oxygen generated from an external source (e.g. oxygen tank), restricting oxygen exposure to only the wound region while reducing the amount of healthy tissue that is exposed to hyper-oxygenation.

One of the latest embodiments of TOT technologies is a handheld system (EPIFLO, Ogenix, Ft. Lauderdale, FL) that concentrates oxygen from the environment and pumps it through a piece of tubing that it feeds into the wound dressing [17,18]. The system is capable of producing oxygen continuously at a rate of 3 mL/h for up to 15 days (at atmospheric pressure), which has been shown to be sufficient for an expedited healing process. This product is definitely an improvement over previous systems, as it allows for patient mobil-

☆ Selected Paper Presented at The 17th International Conference on Solid-State Sensors, Actuators and Microsystems, June 16–20, 2013, Barcelona, Spain.

* Corresponding author. Tel.: +1 562 546 2669; fax: +1 562 546 2669.
E-mail address: ochoam@purdue.edu (M. Ochoa).

http://dx.doi.org/10.1016/j.snb.2014.02.021
0925-4005/

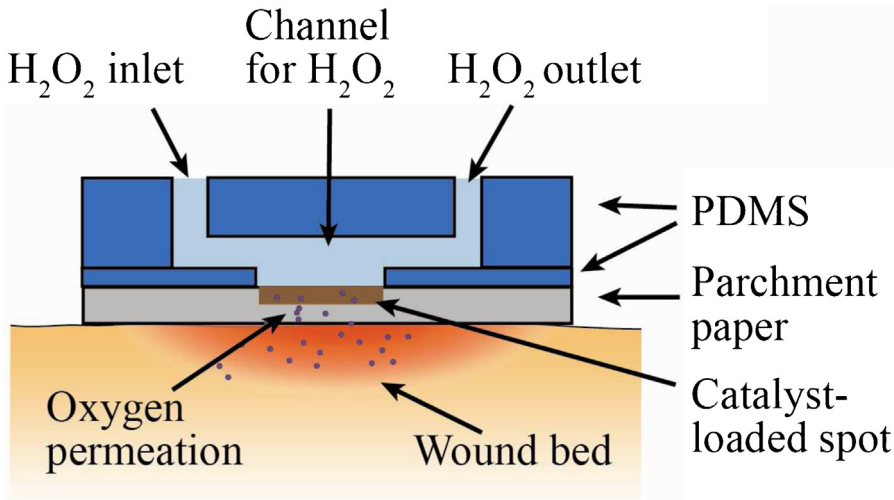

Fig. 1. Cross-sectional schematic of the oxygen-releasing platform at a single catalyst-loaded spot.

ity and limits oxygen exposure to the wound bed. However, the system is still bulky, expensive, and does not provide a means to selectively deliver oxygen to the hypoxic regions within the wound. The treatment of such wounds would greatly benefit from the use of a localized method for oxygen delivery with improved spatial and temporal precision.

In this work, we present a low-cost alternative for continuous O_2 delivery consisting of an inexpensive, paper-based, biocompatible, flexible platform for locally generating and delivering oxygen to selected hypoxic regions. The platform takes advantage of recent developments in the fabrication of flexible microsystems, including the incorporation of paper as a substrate [19–22] and the use of inexpensive laser machining process [23–25]. The use of paper simultaneously provides structural flexibility as well as selective filtering functionality, i.e., it allows for oxygen to pass through while preventing aqueous solutions to reach the tissue. The laser machining enables the precise definition of oxygen generating regions that match the hypoxic wound profile. Together these two technologies enable the development of a low-cost patch/wound-dressing with customized, wound-specific oxygen generating regions.

2. Design and fabrication

The platform consists of a flexible microfluidic network bonded to a parchment paper substrate, as illustrated in Fig. 1. A key feature is the use of a laser-patterned parchment paper as the primary structural/functional substrate. Parchment paper is a hydrophobic material by design; however, it can be ablated using a CO_2 laser to selectively create hydrophilic regions [26]. This technique is applied to define an array of hydrophilic spots. The natural mesh structure of the paper allows the spots to be embedded with chemicals suspended in an aqueous solution. For the present application, the spots are loaded with a chemical catalyst, MnO_2. When H_2O_2 is injected through the microchannel network, it reaches the spot array, and is decomposed by the catalyst, resulting in oxygen generation [27–29]:

$$2H_2O_2 \rightarrow 2H_2O + O_2$$

The generated O_2 diffuses through the paper and oxygenates the wound bed directly below the catalyst spot for as long as H_2O_2 flows in the microchannel. The use of a biocompatible structural material allows the platform to be integrated into commercial wound dressings that are in contact with the wound bed.

The fabrication process of the oxygen generating platform is shown in Fig. 2. It consists of making laser-defined patterns on parchment paper, creating microchannels on a PDMS substrate, and bonding the layers together. The entire procedure is straightforward and requires no complex cleanroom processing. First, the catalyst spot pattern is laser-ablated onto a parchment paper substrate (30 μm thick). The paper is then dipped (1 s) into a 0.1N $KMnO_4$ aqueous solution followed by a dip (1 s) in a 0.1N KI aqueous solution. This results in the deposition of $KMnO_4$ and KI only onto the ablated pattern. The two reactants yield MnO_2 via the following reaction

$$KI(aq) + 2KMnO_4(aq) + H_2O(l) \rightarrow KIO_3(aq) + 2KOH(aq) + 2MnO_2(s).$$

Next, PDMS (polydimethyl siloxane, Dow Corning Sylgard 184) is spin-coated on a silanized silicon wafer and cured on a hotplate (100 °C, 20 min) for a final thickness of 200 μm. The PDMS is transferred onto an acrylic substrate and laser-machined to create through-hole regions with the same pattern as the catalyst. The patterned PDMS is exposed to air plasma (75 W, 1 min) in a plasma etcher (PLASMOD, Tegal Corporation, Richmond, CA), stamped onto uncured PDMS, and partially cured on a hotplate (65 °C, 5 min). Next, the PDMS is bonded to the patterned parchment paper by plasma-treating both materials and bringing them

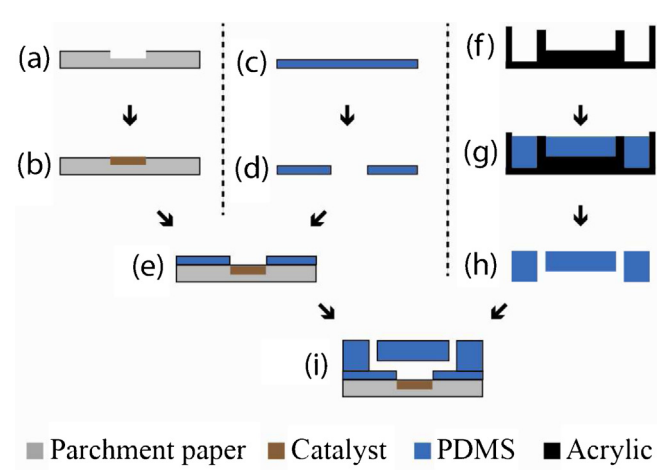

Fig. 2. Fabrication procedure (a) laser-pattern parchment paper, (b) deposit catalyst, (c and d) laser-machine 200 μm thick PDMS, (e) bond paper to PDMS by stamping partially-cured PDMS, (f–h) mold PDMS microchannels, (i) bond the PDMS microchannels to the paper substrate after plasma treatment.

in contact. Finally, 150 μm-deep microchannels are fabricated in PDMS by casting onto a laser-machined acrylic mold, and they are subsequently bonded to the parchment paper structure after plasma treatment.

A modified structure was also fabricated for the PDMS-parchment paper bond strength characterization and measurement of gas permeability through the parchment paper. The structure consisted of a 14 mm × 14 mm × 4 mm piece of PDMS with a circular chamber of 8 mm diameter and 2 mm height. For the bond strength tests, the PDMS chamber was bonded to a piece of parchment paper either (1) directly, (2) with an intermediate layer of partially cured PDMS, or (3) with an intermediate layer of uncured PDMS. In all cases, both surfaces were treated with air plasma (75 W, 1 min), then brought into contact, and finally allowed to completely cure on a hotplate at 65 °C. The best bonding technique (using partially cured PDMS) was then used to fabricate a test device with the same design for characterizing the gas permeability of the parchment paper.

3. Experimental setup

The devices were characterized in terms of the paper-PDMS bond strength, gas permeability, oxygen generation capability, and biocompatibility. The bond strength of the PDMS-paper interface was measured using the modified test devices. A stainless steel needle was used for the fluid connection and its perimeter was sealed with silicone adhesive. A syringe pump was used to pump water into the device at a rate of 250 μL/h while the pressure was measured using a digital pressure gauge (DPG4000, OMEGA Engineering Inc.). The pressure immediately before device failure was recorded. A similar setup was used to assess the permeability of parchment paper to air. A syringe pump was used to pump air into a test PDMS-parchment paper device bonded using partially cured PDMS and plasma. The pressure in the chamber was measured at various gas flow rates and was used to calculate the permeability of the paper substrate.

The fabricated devices were also tested for oxygen generation and permeation across the parchment paper. A syringe pump was used to drive H_2O_2 through the device to induce oxygen generation at the catalyst-loaded spots. A fiber-optic oxygen measurement system (NeoFox, OceanOptics, Dunedin, FL) was used to measure the oxygen concentration on the opposite side of the parchment paper, recording the oxygen level at catalyst-free and catalyst-loaded regions.

The oxygen level at a single spot was also monitored for 30 h to determine the long-term generation rate. This was achieved using a modified oxygen platform with a single channel and a catalyst spot. To measure the oxygen generated at a catalyst spot, a PDMS chamber (8 mm-diameter, 5 mm height, and 3 mm wall thickness) was attached to the paper side of the test device directly covering the catalyst. Next, the fiber optic oxygen sensing probe was inserted into the chamber (through a small opening in the PDMS) and sealed with silicone adhesive. A 3% hydrogen peroxide solution was subsequently pumped though the microchannel at 250 μL/h to generate oxygen at the catalyst location and, hence, in the PDMS chamber. The oxygen concentration in the chamber was monitored over 30 h and used to calculate the average generation rate (total oxygen volume divided by total operation time).

The transport kinetics of the generated oxygen were investigated to determine the maximum hydrogen peroxide flow rate that would permit accurate delivery of oxygen at its generation location. Oxygen generated at a spot must remain at the spot for sufficient time to allow its permeation across the parchment paper; thus, if the peroxide flow rate is too high, the generated oxygen will be transported downstream and may permeate the parchment paper at an unintended location. The effect of the liquid flow rate was determined by measuring the oxygen level (using the same fiber-optic system mentioned above) across the parchment paper at various distances from the point of generation under different flow rates.

To determine the *in vitro* biocompatibility of the parchment paper, 3T3 fibroblast cells with a cell density of 1×10^5 cells/sample were seeded on the surface of the parchment paper. Since the surface of the parchment paper is hydrophobic, a short (1 min) plasma treatment was applied before the cell seeding process. Cells with the same density were seeded onto the parchment paper with catalyst, parchment paper without catalyst, and a standard well plate (as a control). After 6 h, alamar blue assays were carried out to determine the cytotoxicity of the samples. For the alamar blue assays, the cells were cultured for 6 h and subsequently incubated with 500 μL of alamarBlue® (Invitrogen™, Life Technologies, Inc.) solution for 3 h at 37 °C. Next, 100 μL of reduced alamarBlue® solution was transferred into a 96-well plate for optical absorbance measurements at 570 nm (excitation) and 600 nm (emission).

High concentrations of H_2O_2 are known to be toxic to cells [30]; hence, separation of H_2O_2 flow from the cell-seeded region needed to be verified. Assembled PDMS-parchment paper devices were modified to include an additional 200 μm layer of PDMS bonded to the exposed parchment paper. This layer contained through-holes to form wells around the catalyst-loaded parchment paper regions. The wells were used both to contain and culture the cells, as well as to ensure that the cells remained aligned on top of the oxygen-releasing spots throughout the experiment. In this experiment, the devices were first treated with plasma. Then 3T3 fibroblast cells with a density of 5×10^4 cells/sample were seeded on the surface of the devices. Next, a 3% of H_2O_2 solution at a flow rate of 250 μL/h was introduced through the channels for 15 hours. After 15 h of culture time, alamar blue assays were performed to measure cell proliferation. As a control group, we cultured cells on devices without any H_2O_2 flow.

4. Results and discussion

The photographs in Fig. 3 show a fabricated oxygen generation device with four spots loaded with MnO_2. Fig. 3(a and b)

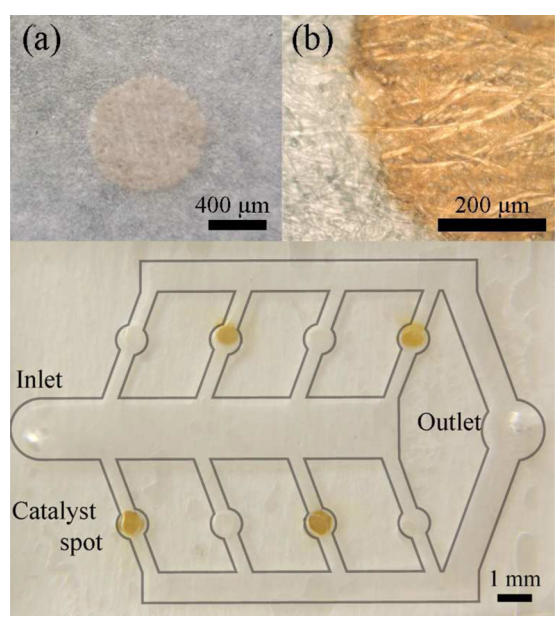

Fig. 3. Photographs of (a) a laser-patterned disk on parchment paper, (b) a magnified view of the disk after loading with catalyst, and (c) top view of a completed device with only four patterned disks (channels are 150 μm deep; overall device thickness is 1.5 mm).

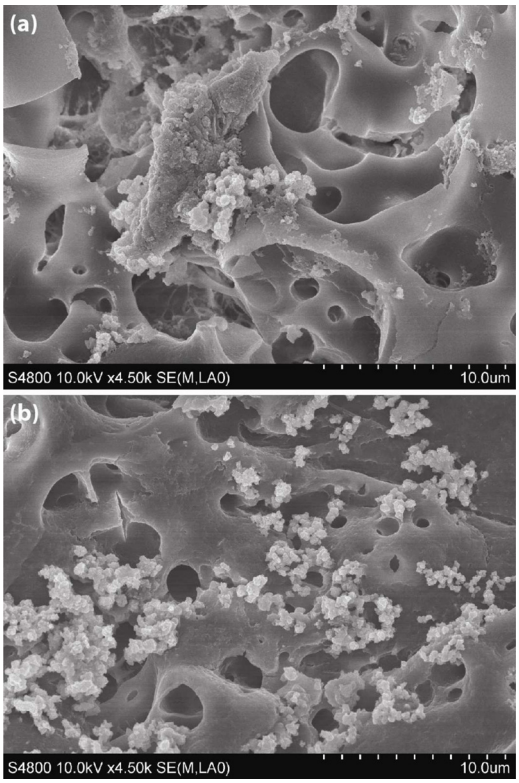

Fig. 4. SEM images of MnO_2 particles in a laser-ablated spot on parchment paper. (a) Catalyst deposited as an aqueous suspension of MnO_2 particles results in large material clumps on the paper surface. (b) Catalyst deposited by on-spot precipitation via the chemical reaction of two aqueous solutions of KI and $KMnO_4$ results in smaller, more uniformly distributed and entrapped particles.

displays the pattern definition capabilities of the process; the laser-ablated spots are clearly defined and their hydrophilicity allows for precise patterning of the catalyst. The spots have a diameter of 800 μm, but smaller (or larger) custom sizes are possible down to the resolution limit of the laser system (125 μm in our case). Fig. 3c presents a device with only four catalyst spots defined on the paper even though the accompanying microfluidic network can support eight spots. Hence, different wound-customized oxygen generating patches can be easily created by simply altering the spot pattern on the paper without requiring modifications of the microfluidics.

Magnified views of a catalyst spot are shown in the SEM images in Fig. 4. In Fig. 4a, an aqueous solution of powder MnO_2 was cast on the spot whereas in Fig. 4b, the same catalyst material was deposited via a chemical reaction of two aqueous reactants (KI, $KMnO_4$). The images show the increased uniformity and smaller particle size achievable with the reaction-deposition approach as opposed to the powder casting method. With the reaction approach, the wicking action of the paper in the catalyst spots absorbs each of the reactants, allowing the catalyst precipitate to be generated within the paper mesh for improved particle entrapment and reduced catalyst washout rate during operation.

The characterization data for the PDMS-parchment paper bond strength is shown in Fig. 5. This test compared the bond strength of parchment paper bonded to PDMS as described in the fabrication section using (1) fully cured PDMS, (2) partially cured PDMS, and (3) uncured PDMS. The results show that a maximum pressure was achieved when bonding the two materials using partially cured PDMS. This method created a bond capable of withstanding up to 323 Torr. During these tests, the parchment paper was also observed to be impermeable to aqueous solutions for pressures below 110 Torr. Hence, the flow of H_2O_2 in the channels was

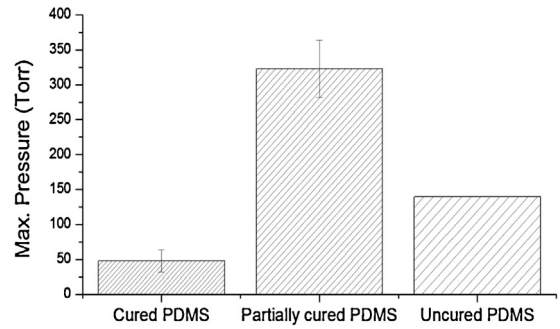

Fig. 5. The PDMS-parchment paper bond strength is highest when bonding using partially-cured PDMS.

not expected to affect cell cultures on the opposite side of the parchment paper as long as the liquid pressure remained below this level.

Fig. 6 shows the gas permeability data for the parchment paper measured using the test device. The pressure (P) versus gas flow rate (Q) data reveals a slope of 0.014 Torr/μL/min. Since the test devices have a parchment paper area (A) of 50.24 mm^2, the gas permeability (κ) of the paper can be computed to be

$$\kappa = \frac{\Delta Q}{\Delta P}\frac{1}{A} \approx 1.42\ \mu L/(\text{Torr mm}^2\ \text{min}).$$

For a maximum pressure of 110 Torr (after which H_2O_2 may permeate through the paper), the paper is suitable for oxygen generation rates of up to about 4.91 μL/min/spot. This value is sufficiently high to allow oxygen permeation at a typical wound oxygen consumption rate of 3 mL/h [15] with only eleven 200-μm diameter spots.

The ability to increase the oxygen level across parchment paper was confirmed with direct oxygen measurements using an optical oxygen sensor positioned 1 mm above the paper surface. An increase of oxygen concentration from 20.9% to 25.6% was observed on the exposed side of the paper for regions with catalyst (Fig. 7). Long-term (30 h) measurements of continuous oxygen generation revealed a constant oxygen generation rate of 0.1 μL O_2/min/mm^2 (Fig. 8). A comparable level of oxygenation (0.3 μL O_2/min/mm^2) has been previously shown to effectively promote epithelial healing in a rabbit ear wound model [12]. Thus, our platform can generate oxygen at a sufficiently high rate to alter the oxygen level in the microenvironment of a wound and improve wound healing. Although the platform would require regular replacement (with an optional new catalyst deposition) throughout the duration of

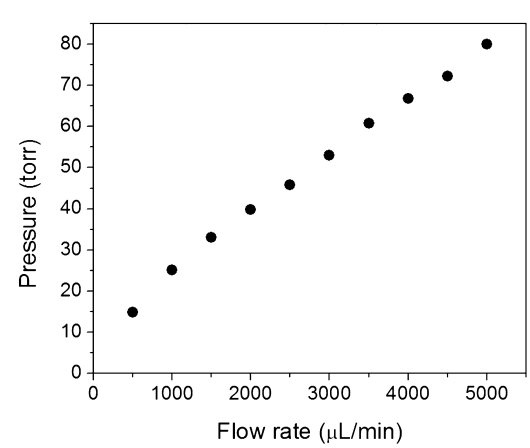

Fig. 6. The gas permeability of parchment paper was determined from the pressure vs. air flow rate profile. Parchment paper dimensions: radius = 4 mm, t = 30 μm.

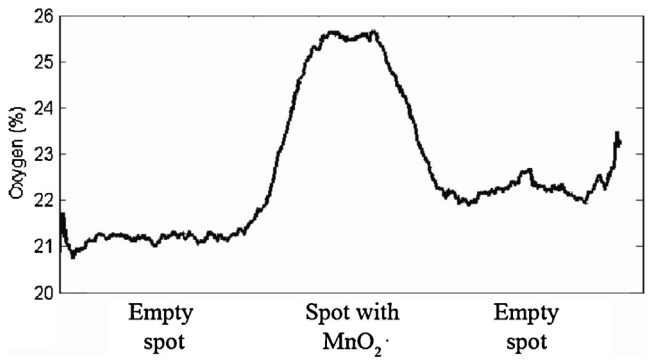

Fig. 7. Partial pressure of oxygen in air at the parchment paper surface opposite the reaction site.

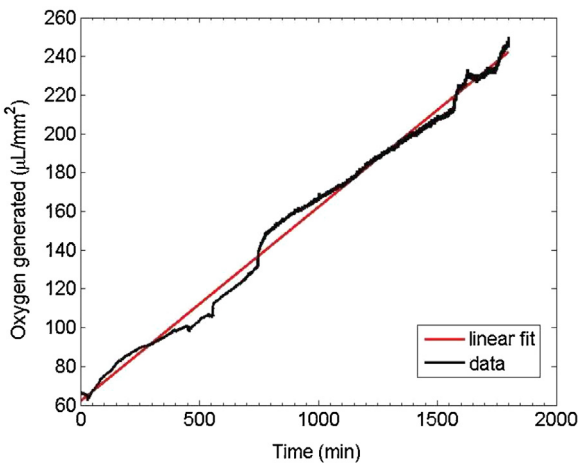

Fig. 8. Long-term (30 h) oxygen generation profile. Oxygen is generated at a rate of 0.1 μL O_2/min/mm^2 when flowing 3% H_2O_2 at 250 μL/h. The peroxide concentration and flow rate can be increased to achieve generation rates that have been clinically proven to effectively promote epithelial healing.

therapy, its replacement schedule (no more than once per day) is no more burdensome than common wound dressings. The rate of oxygenation can be further controlled by varying the number of patterned spots, the amount of catalyst deposited on the spots, and/or the flow rate and concentration of H_2O_2.

The oxygen transport kinetics of the platform for various flow rates are shown in Fig. 9. The plot depicts the level of oxygen as

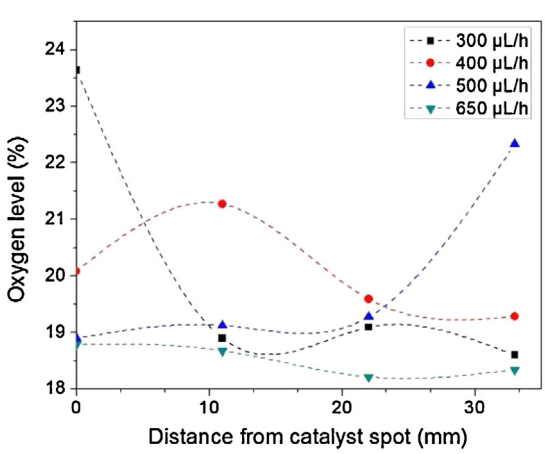

Fig. 9. Oxygen level across parchment paper as a function of the distance from the generation location using various hydrogen peroxide flow rates. Oxygen delivery accuracy is optimum for H_2O_2 flow rates of 300 μL/h or lower.

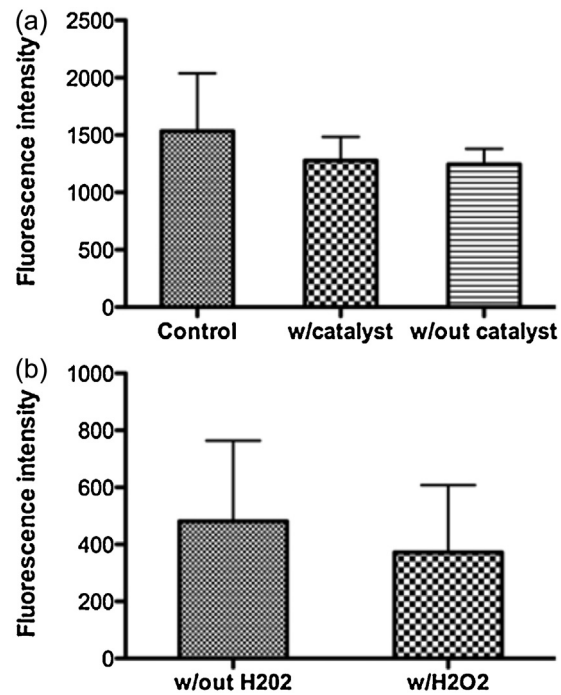

Fig. 10. The results of alamar blue assays of (a) a control sample (standard well plate), parchment paper with catalyst, and patterned parchment paper without catalyst and (b) devices without H_2O_2, and with 3% H_2O_2 at a flow rate of 250 μL/h. For both experiments, 3T3 fibroblast cells were seeded on the surface of the parchment paper or the channel devices ($n = 3$, standard deviation). For the alamar blue assays, the cells were cultured for 6 h and subsequently incubated with 500 μL of alamarBlue® (Invitrogen™, Life Technologies, Inc.) solution for 3 h at 37 °C. Next, 100 μL of reduced alamarBlue® solution was transferred into a 96-well plate for optical absorbance measurements at 570 nm (excitation) and 600 nm (emission). Error bars, ±SD. One-way ANOVA followed by Bonferroni test were performed where appropriate to measure statistical significance.

a function of the downstream distance from the point of oxygen generation for various flow rates of H_2O_2. The data show that for the channels used (rectangular cross-section of 500 μm × 200 μm), a flow rate of 300 μL/h is slow enough to provide generated oxygen with sufficient time to permeate the channel and paper at the generation spot. At higher flow rates, however, cross-paper oxygen levels peak at a location downstream from the generation spot, suggesting that flow rates higher than 300 μL/h would result in excessive lateral transport of oxygen that would prevent accurate localized delivery. Therefore, the oxygen platform exhibits satisfactory performance as long as the H_2O_2 flow rate over a spot is maintained at or below 300 μL/h.

The biocompatibility results for the materials and finished devices are shown in Fig. 10. The alamar blue assay performed for 3T3 cells on parchment paper (Fig. 10a) showed no significant difference between the metabolic activities of cells seeded on the culture dish as a control and that of the cells seeded on the two parchment paper samples, with and without catalyst. These results imply the biocompatibility of both the parchment paper and the catalyst. Similarly, the analyses on the assembled structures with flowing H_2O_2 showed no significant difference in the metabolic activities of the cells, compared to the control (Fig. 10b). This suggests that H_2O_2 does not come into contact with the seeded cells during device operation and implies the biocompatibility of the fabricated oxygen generators.

The overall performance of the oxygen generation platform is adequate for its intended application as a component of a disposable oxygen therapy wound dressings. Future development will focus on practical packaging measures necessary for clinical use. These include its incorporation into a commercial

wound dressing as well as the implementation of an on-board hydrogen peroxide source. The microfluidic design provides a convenient platform for encapsulating H_2O_2 in a small (1–10 mL) pre-pressurized chamber that delivers a continuous flow through the microchannels. For example, a reservoir with dimensions 100 mm × 100 mm × 1 mm would contain enough 3% H_2O_2 solution to generate about 100 mL O_2 (4.41 mol O_2), hence enabling a production rate of 3 mL O_2/h for up to 33 h at atmospheric pressure. The peroxide concentration and/or the reservoir dimensions can be adjusted to optimize the platform size or oxygenation capacity. The oxygen release profile for completely packaged devices will be subsequently evaluated with *in vitro* and/or *in vivo* experiments.

5. Conclusions

We have developed an inexpensive, flexible, paper-based oxygen generation platform for locally generating and delivering oxygen to the microenvironment of chronic wounds. The platform consists of a PDMS microfluidic network bonded to an array of laser-defined (and hence, customizable) MnO_2-loaded hydrophilic spots on an otherwise hydrophobic parchment paper substrate. H_2O_2 is introduced into the PDMS microchannels for the generation of oxygen via catalytic decomposition at the MnO_2 spots. The generated oxygen then permeates through the parchment paper to reach the wound bed. Oxygen generation in the catalyst spots raised the oxygen level on the opposite side of the parchment paper to clinically acceptable levels. An alamarBlue® assay using 3T3 cells revealed that the parchment paper with and without MnO_2 is not cytotoxic and that the fabricated design isolates the seeded cells from H_2O_2 flow during the release of oxygen.

Acknowledgements

The authors thank the staff at the Birck Nanotechnology Center for their support. We also thank Professor Çagri Savran and Dr. Chun-Li Chang for their assistance with laser micromachining. Funding for this research was provided by the National Science Foundation under Grant EFRI-BioFlex #1240443.

References

[1] S. Schreml, R.M. Szeimies, L. Prantl, S. Karrer, M. Landthaler, P. Babilas, Oxygen in acute and chronic wound healing, Br. J. Dermatol. 163 (2010) 257–268.
[2] A.A. Tandara, T.A. Mustoe, Oxygen in wound healing—more than a nutrient, World J. Surg. 28 (2004) 294–300.
[3] T.E. Wright, W.G. Payne, F. Ko, D. Ladizinsky, N. Bowlby, R. Neeley, et al., The effects of an oxygen-generating dressing on tissue infection and wound healing, J. Appl. Res. 3 (2003) 363–370.
[4] G.S. Schultz, R.G. Sibbald, V. Falanga, E.A. Ayello, C. Dowsett, K. Harding, et al., Wound bed preparation: a systematic approach to wound management, Wound Repair Regen. 11 (2003) 1–28.
[5] A. Namiki, E. Brogi, M. Kearney, E.A. Kim, T. Wu, T. Couffinhal, et al., Hypoxia induces vascular endothelial growth factor in cultured human endothelial cells, J. Biol. Chem. 270 (1995) 31189–31195.
[6] C.K. Sen, Wound healing essentials: let there be oxygen, Wound Repair Regen. 17 (2010) 1–18.
[7] J.A. Flegg, H.M. Byrne, D.L.S. McElwain, Mathematical model of hyperbaric oxygen therapy applied to chronic diabetic wounds, Bull. Math. Biol. 72 (2010) 1867–1891.
[8] P.M. Tibbles, J.S. Edelsberg, Hyperbaric-oxygen therapy, N. Engl. J. Med. 334 (1996) 1642–1648.
[9] M.A. Howard, R. Asmis, K.K. Evans, T. aMustoe, Oxygen and wound care: A review of current therapeutic modalities and future direction, Wound Repair Regen. (2013) 1–9.
[10] B.M. Smith, L.D. Desvigne, J.B. Slade, J.W. Dooley, D.C. Warren, Transcutaneous oxygen measurements predict healing of leg wounds with hyperbaric therapy, Wound Repair Regen. 4 (1996) 224–229.
[11] C.L. Hess, M.A. Howard, C.E. Attinger, A review of mechanical adjuncts in wound healing: hydrotherapy, ultrasound, negative pressure therapy, hyperbaric oxygen, and electrostimulation, Ann. Plast. Surg. 51 (2003) 210–218.
[12] H.K. Said, J. Hijjawi, N. Roy, J. Mogford, T. Mustoe, Transdermal sustained-delivery oxygen improves epithelial healing in a rabbit ear wound model, Arch. Surg. 140 (2005) 998–1004.
[13] G.M. Gordillo, R. Schlanger, W. a Wallace, V. Bergdall, R. Bartlett, C.K. Sen, Protocols for topical and systemic oxygen treatments in wound healing, Methods Enzymol. 381 (2004) 575–585.
[14] D.M. Castilla, Z.-J. Liu, O.C. Velazquez, Oxygen implications for wound healing, Adv. Wound Care. 1 (2012) 225–230.
[15] D. Kemp, M. Hermans, An evaluation of the efficacy of Transdermal Continuous Oxygen Therapy in patients with recalcitrant diabetic foot ulcer, J. Diabet. Foot Complicat. 3 (2011) 6–12.
[16] G.M. Gordillo, S. Roy, S. Khanna, R. Schlanger, S. Khandelwal, G. Phillips, et al., Topical oxygen therapy induces vascular endothelial growth factor expression and improves closure of clinically presented chronic wounds, Clin. Exp. Pharmacol. Physiol. 35 (2008) 957–964.
[17] P. Banks, C. Ho, A novel topical oxygen treatment for chronic and difficult-to-heal wounds: case studies, J. Spinal Cord Med. 31 (2008) 297–301.
[18] Ogenix, EPIFLO® Transdermal Continuous Oxygen Therapy [TCOT] for Wound Healing, 2012.
[19] A. Russo, B.Y. Ahn, J.J. Adams, E.B. Duoss, J.T. Bernhard, J.A. Lewis, Pen-on-paper flexible electronics, Adv. Mater. 23 (2011) 3426–3430.
[20] C.-M. Cheng, A.D. Mazzeo, J. Gong, A.W. Martinez, S.T. Phillips, N. Jain, et al., Millimeter-scale contact printing of aqueous solutions using a stamp made out of paper and tape, Lab Chip (2010) 3201–3205.
[21] A.W. Martinez, S.T. Phillips, M.J. Butte, G.M. Whitesides, Patterned paper as a platform for inexpensive, low-volume, portable bioassays., Angew, Chem. Int. Ed. Engl. 46 (2007) 1318–1320.
[22] Z. Ding, P. Wei, G. Chitnis, B. Ziaie, Ferrofluid-impregnated paper actuators, J. Microelectromech. Syst. 20 (2011) 59–64.
[23] M. Ochoa, G. Chitnis, B. Ziaie, Laser-micromachined cellulose acetate adhesive tape as a low-cost smart material, J. Polym. Sci. Part B Polym. Phys. 51 (2013) 1263–1267.
[24] H. Klank, J.P. Kutter, O. Geschke, CO(2)-laser micromachining and back-end processing for rapid production of PMMA-based microfluidic systems, Lab Chip 2 (2002) 242–246.
[25] G. Chitnis, B. Ziaie, Waterproof active paper via laser surface micropatterning of magnetic nanoparticles, ACS Appl. Mater. Interfaces 4 (2012) 4435–4439.
[26] G. Chitnis, Z. Ding, C.-L. Chang, C.A. Savran, B. Ziaie, Laser-treated hydrophobic paper: an inexpensive microfluidic platform, Lab Chip 11 (2011) 1161–1165.
[27] S.-H. Do, B. Batchelor, H.-K. Lee, S.-H. Kong, Hydrogen peroxide decomposition on manganese oxide (pyrolusite): kinetics, intermediates, and mechanism, Chemosphere 75 (2009) 8–12.
[28] D.B. Broughton, R.L. Wentworth, Mechanism of decomposition of hydrogen peroxide solutions with manganese dioxide. I, J. Am. Chem. Soc. 69 (1947) 741–744.
[29] D.B. Broughton, R.L. Wentworth, M.E. Laing, Mechanism of decomposition of hydrogen peroxide solutions with manganese dioxide. II, J. Am. Chem. Soc. 69 (1947) 744–747.
[30] R.H. Burdon, Superoxide and hydrogen peroxide in relation to mammalian cell proliferation, Free Radic. Biol. Med. 18 (1995) 775–794.

Biographies

Manuel Ochoa received the B.S. degree in electrical engineering from the California Institute of Technology, Pasadena, CA in 2009 and the M.S. degree in electrical and computer engineering from Purdue University, West Lafayette, IN in 2012. He is currently pursuing a Ph.D. degree in electrical and computer engineering at Purdue University. Since 2009 he has been a research assistant with the Ziaie Biomedical Microdevices Laboratory at Purdue. His research focuses on the integration of inexpensive commercial materials for the development low-cost, multifunctional, microsystem platforms for biomedical applications, including transdermal drug delivery and dermal wound healing.

Rahim Rahimi received the B.S. degree in electrical engineering from the Iran University of Science and Technology, in 2008. He is currently working toward the Ph.D. degree in electrical and computer engineering at Purdue University, West Lafayette, IN. His current research interests include drug delivery, microfluidic, implantable devices, flexible electronics, electrochemical sensors, biomedical sensors and biomedical applications of microelectromechanical systems.

Tiffany L. Huang is a senior undergraduate student pursuing a B.S. degree in Bioengineering at Rice University. During the summer of 2013, she conducted research at Purdue University under the guidance of Dr. Babak Ziaie as part of the Summer Undergraduate Research Fellowships (SURF) program. She plans to pursue an M.D. degree at Case Western Reserve University School of Medicine beginning in the fall of 2014.

Neslihan Alemdar is currently assistant professor in the Department of Chemical Engineering at Marmara University, Istanbul, Turkey. Alemdar received her Ph.D. degree from Istanbul Technical University in Chemical Engineering in 2009. During 2011–2013, she worked as a Post-Doctoral Research Fellow at Harvard-MIT Health Sciences and Technology Institute & Massachusetts Institute of Technology (Harvard-MIT) in Tissue Engineering Field (USA). She previously worked as a Research and Improvement Engineer at Medicine and Chemical Materials Company in the Research and Improvements Department, and she has 2 years of industrial experience at Plastics Company in the Total Quality Management Department, Istanbul, Turkey. Her research interests are focused on the synthesis and characterization

of smart polymers and their applications for different areas, especially the fabrication of hydrogel for tissue engineering applications and drug delivery systems.

Ali Khademhosseini is an associate professor of Medicine and Health Sciences and Technology at Harvard-MIT's Division of Health Sciences and Technology and the Harvard Medical School. His research is based on developing micro and nano-scale technologies to control cellular behavior with particular emphasis in developing microscale biomaterials and engineering systems for tissue engineering and drug delivery. He has edited multiple books/journal special issues and is an author on ~300 journal articles, ~50 book chapters/editorials, over 200 abstracts, and 15 patent/disclosure applications. He has received numerous awards including the TR35 by the Technology Review Magazine, the Coulter Foundation Early Career, NSF Career, the Presidential Early Career Award for Scientists and Engineers (PECASE), and ONR Young Investigator as well as early career awards including the Colburn Award (AIChE), the Y.C. Fung Award (ASME) and the EMBS early career award (IEEE). He received his PhD in bioengineering from MIT (2005), and MASc (2001) and BASc (1999) degrees from University of Toronto both in chemical engineering.

Mehmet R. Dokmeci received the B.S. (with distinction) and M.S. degrees from the University of Minnesota, Minneapolis, and the Ph.D. degree from the University of Michigan, Ann Arbor all in electrical engineering. His dissertation was on hermetic encapsulation of implantable microsystems for chronic use in living systems. He is currently an Instructor at Brigham and Women's Hospital, Harvard Medical School, Boston, MA. He was previously a faculty member at Northeastern University, Boston, and has 4 years of industrial experience with Corning-Intellisense Corporation, Wilmington, MA. He is the author or co-author of 56 peer-reviewed technical journal articles, 98 conference publications, has five invited book chapters and four patents. His current research interests include micro- and nanofabrication and their applications to biomedical sensors and devices and tissue engineering. Dr. Dokmeci is a member of the AAAS, IEEE, ACS, BMES and MRS.

Babak Ziaie received his doctoral degree in Electrical Engineering from the University of Michigan in 1994. From 1995 to 1999 he was a postdoctoral-fellow and an assistant research scientist at the Center for Integrated Microsystems (CIMS) of the University of Michigan. He subsequently joined the Electrical and Computer Engineering Department of the University of Minnesota as an assistant professor (1999–2004). Since January 2005, he has been with the School of Electrical and Computer Engineering at Purdue University where he is currently a professor. His research interests are related to the biomedical applications of MEMS and Microsystems (BioMEMS).